Resonant x-ray scattering study on multiferroic BiMnO₃

C.-H. Yang,[1] J. Koo,[1] C. Song,[1] T. Y. Koo,[2] K.-B. Lee,[1] and Y. H. Jeong[1]

[1]*Department of Physics & Electron Spin Science Center, Pohang University of Science and Technology, Pohang, Korea*
[2]*Pohang Accelerator Laboratory, Pohang University of Science and Technology, Pohang, Korea*
(Received 9 March 2006; published 20 June 2006)

Resonant x-ray scattering is performed near the Mn K-absorption edge for an epitaxial thin film of BiMnO₃. The azimuthal angle dependence of the resonant (003) peak (in monoclinic indices) is measured with different photon polarizations; for the $\sigma \rightarrow \pi'$ channel a threefold symmetric oscillation is observed in the intensity variation, while the $\sigma \rightarrow \sigma'$ scattering intensity remains constant. These features are accounted for in terms of the peculiar ordering of the manganese $3d$ orbitals in BiMnO₃. It is demonstrated that the resonant peak persists up to 770 K with an anomaly around 440 K; these high and low temperatures coincide with the structural transition temperatures, seen in bulk, with and without a symmetry change, respectively. A possible relationship of the orbital order with the ferroelectricity of the system is presented.

I. INTRODUCTION

Recently multiferroics with the coexistence of ferroelectricity and magnetism have been intensively studied not only due to potential applications but also from basic interest.[1] In particular, BiMnO₃ is regarded as a true multiferroic material with both ferromagnetism and ferroelectricity. BiMnO₃ possesses a distorted perovskite structure with monoclinic symmetry due to highly polarizable bismuth ions and Jahn-Teller (JT) active manganese ions. Its magnetic moment certainly arises from the $3d^4$ electrons of Mn³⁺ ion, while the ferroelectric polarization does from the Bi $6s^2$ lone pair.[2] The saturated magnetization for a polycrystalline sample was reported to be 3.6 μ_B/Mn and the ferromagnetic transition temperature 105 K.[3] While the ferroelectric remanent polarization of BiMnO₃ was measured to be 0.043 μC/cm² at 200 K for a polycrystalline sample,[4] there seems to be no consensus on the ferroelectric transition temperature T_{FE}. Moreira dos Santos *et al.*, for example, reported $T_{FE} \approx 450$ K where a reversible structural transition occurs without a symmetry change;[4] however, Kimura *et al.* suggested $T_{FE} \approx 750$–770 K where a centrosymmetric-noncentrosymmetric structural transition occurs.[5]

In BiMnO₃ orbital degrees of freedom are also active besides magnetic and electric ones; the half-filled e_g level of Mn³⁺ ion induces the JT distortion and an anisotropic charge distribution with the $3d_{3z^2-r^2}$ orbital prevails locally. Then long range orbital order, which is compatible with the structure, would exist in the system. The detailed structure of BiMnO₃ at room temperature was investigated by neutron powder diffraction and the compatible orbital order was proposed.[6] It is noted that no noticeable structural change associated with the ferromagnetic transition was observed. Regarding the orbital order in BiMnO₃, there remain unresolved issues such as the temperature dependence of the degree of ordering at high temperatures and the determination of the transition temperature itself, T_0. Moreover, the relationship between the ferroelectricity and the orbital order in this multiferroic compound is clearly of interest.

In order to address these issues we took advantage of resonant x-ray scattering (RXS) which can probe local environments of a specific element. RXS occurs as a second-order process by first exciting a core electron into an empty valence state, as the incident photon energy is tuned to an absorption edge, and then de-exciting the electron back to the original state. Direct involvement of the valence state in the scattering process usually gives rise to enhanced sensitivity to anisotropic charge distributions, and the atomic scattering factor is no longer a scalar but takes a tensorial form called anisotropic tensor susceptibility (ATS). ATS then allows reflections at some of the normally forbidden positions. Pioneering works regarding ATS were done in the 1980s,[7–11] and more recently Murakami *et al.* successfully applied RXS to several orbital ordered compounds.[12,13] Here we wish to present detailed RXS measurements for BiMnO₃ to reveal a role of the orbital order in this important multiferroic compound. The energy profile, azimuthal angle dependence, and temperature dependence of an ATS reflection peak will be presented and discussed.

II. EXPERIMENTALS

In order to carry out RXS measurements single crystalline samples are needed, but BiMnO₃ is notoriously difficult to synthesize in a single crystalline form. Thus we resorted to epitaxial films; an epitaxial film of BiMnO₃ was grown on a SrTiO₃(111) substrate (cubic Miller indices) by the pulsed laser deposition technique. The thickness of the film was approximately 40 nm. The detailed growth conditions and structural characterizations are presented elsewhere.[14] The crystal structure of the thin film was still monoclinic as in bulk. The growth direction or surface-normal direction, which is parallel to the [111] direction of the substrate, is perpendicular to the monoclinic *ab* plane. Note that with this orientation the modulation vector of the orbital ordering of BiMnO₃ is along the surface-normal. (See the following.) Thus the orientation of the film was deliberately chosen in order to make the axis of azimuthal rotation (direction of the scattering vector) coincide with the surface-normal, so that azimuthal scans are easily performed. Resonant x-ray scattering experiments were performed on a four-circle diffractometer installed at the 3C2 beam line in the Pohang Light
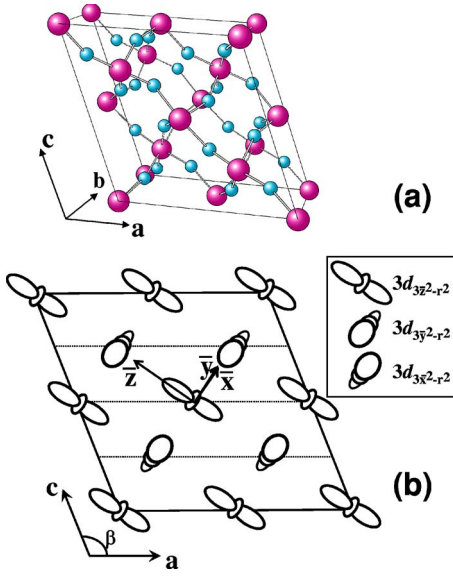
FIG. 1. (Color online) (a) The monoclinic cell of $BiMnO_3$. Larger spheres represent manganese ions and smaller ones oxygen ions. Bismuth ions are omitted for simplicity. The crystallographic axes for the monoclinic unit cell are denoted with a, b, and c. The Mn ab planes are located at $z=0$, $z=\frac{1}{4}-\epsilon$, $z=\frac{1}{2}$, and $z=\frac{3}{4}+\epsilon$ along the c axis. ϵ denotes a small displacement. The angle (β) between the a and c axes is approximately $110°$. (b) The orbital ordering in the unit cell. The axes for the pseudocubic cell are represented by $\bar{x}$, $\bar{y}$, and $\bar{z}$. The ab planes at $z=0$ and $z=\frac{1}{2}$ contain the manganese ions with the orbital ($d_{3\bar{z}^2-r^2}$) elongated to the pseudocubic $\bar{z}$ axis, while the ab planes at $z=\frac{3}{4}+\epsilon$ and $z=\frac{1}{4}-\epsilon$ do only $d_{3\bar{y}^2-r^2}$ and $d_{3\bar{x}^2-r^2}$ orbitals, respectively.

Source. The photon energy near Mn K-edge was calibrated using a manganese foil and the resolution was about 2 eV. The σ polarized photon (electric field perpendicular to the scattering plane) was injected after being focused by a bent mirror and monochromatized by a Si(111) double crystal. The linearly polarized σ' (electric field perpendicular to the scattering plane) and π' (electric field in the scattering plane) components of scattered photons were separated with a flat pyrolithic graphite crystal with the scattering angle of $69°$ for the Mn K-edge.

III. CRYSTAL STRUCTURE AND STRUCTURE FACTOR OF $BiMnO_3$

From the neutron powder diffraction with bulk samples at room temperature the space group (monoclinic $C2$) and local bond lengths and angles of $BiMnO_3$ were all determined,[6] and it turned out that this monoclinic structure is maintained in thin films.[14] The crystallographic unit cell is illustrated in Fig. 1(a). Note that a, b, and c denote the crystallographic axes (and the lattice parameters) for the monoclinic unit cell, and $\bar{x}$, $\bar{y}$, and $\bar{z}$ represent the axes of the perovskite pseudocubic cell. The structure also determines the orientation of JT-distorted MnO_6's and the compatible ordered pattern of the e_g orbitals of Mn^{3+}. The monoclinic ab planes at $z=0$ and $z=\frac{1}{2}$ contain manganese ions with the e_g orbital elongated to the pseudocubic $\bar{z}$ axis $d_{3\bar{z}^2-r^2}$, while the orbitals in the ab

planes at $z=\frac{3}{4}+\epsilon$ and $z=\frac{1}{4}-\epsilon$ are of type $d_{3\bar{y}^2-r^2}$ and $d_{3\bar{x}^2-r^2}$, respectively. Here z denotes the coordinate along the c axis and ϵ designates a small displacement. As illustrated in Fig. 1(b), this orbital order is rather peculiar in the sense that each plane parallel to the ab plane and separated by $c/4$ contains only one kind of the e_g orbital within the plane and the stacking sequence goes as $d_{3\bar{z}^2-r^2}/d_{3\bar{x}^2-r^2}/d_{3\bar{z}^2-r^2}/d_{3\bar{y}^2-r^2}/\ldots$ ($\equiv Z/X/Z/Y/\ldots$). This long range orbital order corresponds to the superstructure of the system, and the periodic arrangement of the anisotropic charge distributions would give rise to measurable intensities at $(00L)$ ATS reflections with odd L where normal charge scattering is almost absent (not completely absent because of nonzero ϵ).

With the crystal structure just described the structure factor $\mathcal{S}_{(00L)}$ for $BiMnO_3$ (odd L), can be written as

$$\mathcal{S}_{(00L)} = 2\mathcal{F}_z e^0 + 2\mathcal{F}_x e^{i2\pi L(1/4-\epsilon)} + 2\mathcal{F}_z e^{i2\pi L1/2} + 2\mathcal{F}_y e^{i2\pi L(3/4+\epsilon)}$$
$$+ S(\text{Bi,O}), \tag{1}$$

where $\mathcal{F}_x$, $\mathcal{F}_y$, and $\mathcal{F}_z$ represent the ATS of the manganese ion with anisotropic e_g orbitals elongated along $\bar{x}$, $\bar{y}$, and $\bar{z}$, respectively, and $S(\text{Bi,O})$ is symbolic of the contribution of Thomson scattering (normal charge scattering) due to bismuth and oxygen ions. $\mathcal{F}_z$, for example, may be written, based on the pseudocubic axes shown in Fig. 1, as follows:

$$\mathcal{F}_z = \begin{pmatrix} f_\perp & 0 & 0 \\ 0 & f_\perp & 0 \\ 0 & 0 & f_\parallel \end{pmatrix}, \tag{2}$$

where $f_\perp$ and $f_\parallel$ stand for the resonant scattering amplitude with photon polarization perpendicular and parallel to the e_g elongation direction, respectively.

Then Eq. (1) becomes

$$\mathcal{S}_{(00L)} \simeq \underbrace{2(-1)^{(L-1)/2} i f_\Delta \begin{pmatrix} 1 & 0 & 0 \\ 0 & -1 & 0 \\ 0 & 0 & 0 \end{pmatrix}}_{\text{ATS contribution}}$$
$$+ \underbrace{8\pi L(-1)^{(L-1)/2} \epsilon f_{\text{Mn}} + S(\text{Bi,O})}_{\text{Thomson scattering}}, \tag{3}$$

where f_{Mn} denotes the isotropic part of the scattering factor of manganese, and f_Δ ($\equiv f_\parallel - f_\perp$) denotes the anisotropic portion.

Note that these $(00L)$ reflections with odd L are allowed even in the absence of resonant scattering because the slight displacement ϵ of Mn ions from the exact position prohibits perfect cancellation of the various contributions. $S(\text{Bi,O})$ in Eq. (1) probably also contributes. ATS reflections are usually so small that the observation of RXS is normally difficult in the presence of a background. The anomalous ATS reflections from the $BiMnO_3$ film, however, were measurable because the charge scattering background at the $(00L)$ peaks turned out to be reduced by a factor of 10^{-5} compared to the intensity of the fundamental (004) peak.
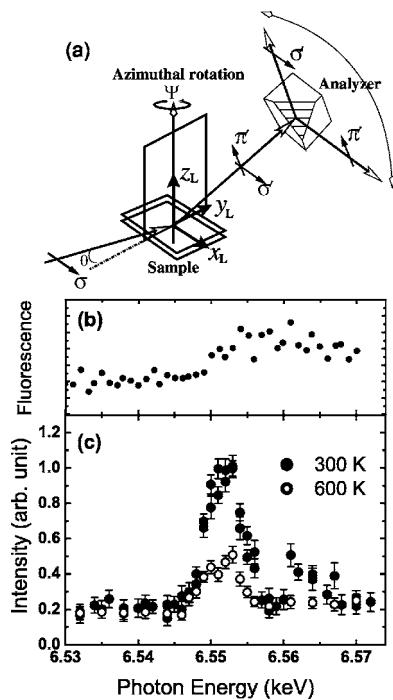
FIG. 2. (a) The experimental configuration for resonant x-ray scattering. σ, σ', and π' represent the polarization of the incident and scattered photons. A flat pyrolithic graphite crystal is used as an analyzer. The Cartesian coordinate ($x_L y_L z_L$) represents the laboratory frame. (b) The fluorescence data represent the Mn K absorption edge. These are collected at 300 K. (c) The energy profiles for the (003) peak measured without an analyzer crystal. The integrated intensities were not corrected for absorption and were obtained at $\psi = 0$.

IV. RESONANT X-RAY SCATTERING

In Fig. 2(a) schematically shown is the experimental configuration for RXS. Again σ, σ', and π' represent the polarization of the incident and scattered photons. Azimuthal rotation and analyzer configuration are also indicated in the figure. The fluorescence was measured as a function of photon energy to determine the Mn K absorption edge. The absorption from the manganese ion results in the uprise of fluorescence above 6.55 keV indicating the Mn K absorption edge as presented in Fig. 2(b). The integrated intensity of the (003) reflection was measured as a function of photon energy as shown in Fig. 2(c). As expected from the resonant nature, the intensity is sharply enhanced at 6.552 keV in contrast to the normal charge scattering intensity which would decrease instead from absorption. Note that at off-resonance energies, appreciable integrated intensity remains, instead of decaying to zero, as a result of normal charge scattering described earlier. Another interesting point is that, as shown in the two energy profiles at different temperatures (300, 600 K), the resonant contribution decreases with temperature in contrast to the off-resonant part which remains nearly constant.

Even if the peak occurred at the expected position in the reciprocal space, this fact alone may not be sufficient to conclude that orbital ordering is indeed the origin of the scattering. The hallmark of the resonant scattering due to orbital ordering would be the polarization dependence and azimuthal variation of the peak intensity. In contrast to conventional x-ray scattering which neither depends on the azimuthal angle nor shows polarization conversion, resonant scattering would exhibit the characteristic oscillations, depending on the photon polarization, with respect to the azimuthal angle, i.e., the rotation angle around the scattering vector. Thus in order to further confirm the orbital order as the origin of this resonant reflection, the azimuthal angle dependence and polarization analysis were carried out. Figure 3 presents the azimuthal angle dependence of the (003) integrated intensity normalized with the fundamental (004) peak intensity in order to remove sample-shape effects. The zero of the azimuthal angle ψ is defined when $\mathbf{k}_i \times \mathbf{k}_f$ coincides with the $+b$ axis. $\mathbf{k}_i$ and $\mathbf{k}_f$, of course, represent the propagation vector of incident and scattered beams, respectively. For the $\sigma \rightarrow \pi'$ channel, a clear threefold oscillation is observed, while the intensity does not exhibit any azimuthal dependence for $\sigma \rightarrow \sigma'$. No doubt this polarization dependence and the threefold oscillation seen in the $\sigma \rightarrow \pi'$ channel are due to orbital ordering. It is noted, however, that these results are not trivially connected to the orbital order of $BiMnO_3$. What is required is one further step of taking into consideration the effects of twins which always exist in the film; the detailed accounts are given in a separate section which follows.

The temperature variation of the orbital order was elucidated by measuring the monoclinic (003) integrated intensities at two different photon energies, 6.532 and 6.552 keV, as shown in Fig. 4. While the intensity at off-resonance energy 6.532 keV is solely due to Thomson scattering (normal charge scattering) and constitutes a background, the RXS intensity at 6.552 keV is caused by the ATS reflection in addition to the background. Note that the off-resonance integrated intensity shows a normal behavior, i.e., decreases with temperature due to thermal vibrations, and will disappear at the structural phase transition point where the monoclinic structure does. The temperature profile of the RXS data shows two distinct features: one is that the peak intensity decreases rather rapidly with temperature and van-
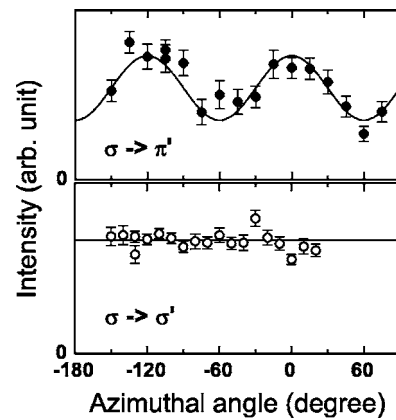

FIG. 3. The azimuthal angle dependence of the (003) integrated intensity for the two channels: $\sigma \rightarrow \pi'$ and $\sigma \rightarrow \sigma'$. The lines were obtained from the calculation of resonant x-ray scattering based on the orbital ordering. See the text.
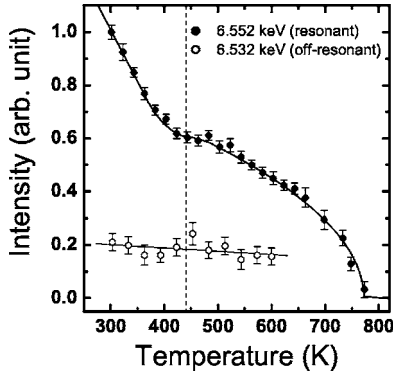
FIG. 4. The (003) integrated intensities are plotted as a function of temperature at two different photon energies. The intensities were collected at $\psi = 0$. The off-resonant intensity constitutes the background. The resonant x-ray scattering intensity at photon energy 6.552 keV is due to orbital ordering, and disappears around 770 K. The dashed line indicates 440 K, where an abrupt increase in the resonant intensity seems to start when temperature is reduced. Solid lines are a guide for the eye.

ishes around 770 K where the centrosymmetric-noncentrosymmetric structural phase transition was seen in bulk. The other is that an anomaly in the temperature variation appears around 440 K, below which there is a sudden upturn in the slope. The former feature proves that the orbital order also vanishes concurrently with the structural phase transition.[5] The lower temperature 440 K coincides with the transition temperature found also in bulk; in this case the phase transition involved is the one without a symmetry change. It is pointed out that the background intensity does not show any abnormal behavior around 440 K and therefore the anomaly is necessarily related to the orbital ordering. These two temperatures are currently under controversy as a point below which ferroelectricity first appears. At high temperatures, it should be noted, it is not trivial at all to prove ferroelectricity of a material. At any rate, the present RXS results reveal that there is a strong connection between the ferroelectricity and orbital order in $BiMnO_3$. Of course, the orbital order also determines exchange interactions and consequently magnetic ordering.

V. CALCULATION OF AZIMUTHAL ANGLE DEPENDENCE

The azimuthal angle dependence of the scattering intensity from the anomalous part proportional to $2(-1)^{(L-1)/2}i$ of Eq. (3) can be calculated for the experimental configuration shown in Fig. 2(a). The conversion matrix ($\mathcal{V}$) from the laboratory frame ($x_L y_L z_L$) to the pseudocubic crystallographic frame ($\overline{xyz}$) is given by

$$\mathcal{V} = \frac{1}{\sqrt{6}}\begin{pmatrix} -\sqrt{3} & -1 & \sqrt{2} \\ \sqrt{3} & -1 & \sqrt{2} \\ 0 & 2 & \sqrt{2} \end{pmatrix}. \quad (4)$$

The polarization vector of the σ, σ', and π' polarizations under azimuthal rotation by the amount of ψ can be written in the laboratory frame as follows:

$$|\sigma\rangle_\psi = |\sigma'\rangle_\psi = \mathcal{R}(\psi)\begin{pmatrix} 1 \\ 0 \\ 0 \end{pmatrix}, \quad (5)$$

$$|\pi'\rangle_\psi = \mathcal{R}(\psi)\begin{pmatrix} 0 \\ -\sin\theta \\ \cos\theta \end{pmatrix}, \quad (6)$$

where θ ($\equiv 2\theta/2$) is the Bragg angle, and $\mathcal{R}(\psi)$ is the azimuthal rotation matrix given by

$$\mathcal{R}(\psi) = \begin{pmatrix} \cos\psi & -\sin\psi & 0 \\ \sin\psi & \cos\psi & 0 \\ 0 & 0 & 1 \end{pmatrix}. \quad (7)$$

From these quantities the scattering intensity caused by ATS with σ as the polarization of the incident photons is easily calculated for the two channels, $\sigma \to \sigma'$ and $\sigma \to \pi'$:

$$I_{\sigma \to \sigma', \pi'} = \left| \langle \sigma', \pi' |_\psi \mathcal{V}^\dagger \begin{pmatrix} 2f_\Delta & 0 & 0 \\ 0 & -2f_\Delta & 0 \\ 0 & 0 & 0 \end{pmatrix} \mathcal{V} |\sigma\rangle_\psi \right|^2. \quad (8)$$

Simplifying this equation yields the scattering intensities as

$$I_{\sigma \to \sigma'} = \tfrac{4}{3} f_\Delta^2 \sin^2 2\psi, \quad (9)$$

$$I_{\sigma \to \pi'} = \tfrac{4}{3} f_\Delta^2 (\sqrt{2}\cos\theta\cos\psi + \cos 2\psi \sin\theta)^2. \quad (10)$$

There is one more factor to be considered before comparison with the experimental data is attempted, that is, the existence of twins has to be taken into account. The films grown on $SrTiO_3(111)$ would include three kinds of stacking sequences of orbitals, i.e., Z/X/Z/Y/..., X/Y/X/Z/..., and Y/Z/Y/X/.... Note that the growth direction, which is the cubic [111] direction, is perpendicular to monoclinic (001) or ab planes. Thus the measured intensities would be the ones obtained after averaging for the twins:

$$I_{\sigma \to \sigma'}^{\text{avr}} = \tfrac{2}{3} f_\Delta^2, \quad (11)$$

$$I_{\sigma \to \pi'}^{\text{avr}} = \frac{f_\Delta^2}{3}(3 + \cos 2\theta + 2\sqrt{2}\sin 2\theta \cos 3\psi). \quad (12)$$

After twin averaging, the calculated expressions as a function of ψ agree with the experimental results depicted in Fig. 3. The data for the $\sigma \to \sigma'$ channel do not show any ψ dependence, whereas for the $\sigma \to \pi'$ channel a characteristic threefold symmetry is exhibited.

VI. CONCLUSIONS

The resonant x-ray scattering technique was used with epitaxial thin films to probe the orbital ordering of a multiferroic compound, $BiMnO_3$. ATS reflection was observed at (003) in the reciprocal space as expected, and the characteristic threefold oscillation showed up as a function of

azimuthal angle. The experimental results agree with the calculation based on the orbital ordering when twin effects are taken into account. The peak intensity was followed as a function of temperature to high temperatures; it rapidly decreases with temperature and disappears at $T_0 \approx 770$ K. Thus orbital ordering occurs concurrent with the centrosymmetric-noncentrosymmetric structural phase transition seen in bulk. The peak intensity also shows an anomaly at 440 K, where again a phase transition was observed in bulk. Although there is no consensus about the ferroelectric phase transition point in $BiMnO_3$, being either 440 or 770 K, the orbital or-

dering is closely connected to the ferroelectricity in the system in either case.

[1] M. Fiebig, J. Phys. D **38**, R123 (2005), and references therein.

[2] N. A. Hill and K. M. Rabe, Phys. Rev. B **59**, 8759 (1999).

[3] H. Chiba, T. Atou, and Y. Syono, J. Solid State Chem. **132**, 139 (1997).

[4] A. Moreira dos Santos, S. Parashar, A. R. Raju, Y. S. Zhao, A. K. Cheetham, and C. N. R. Rao, Solid State Commun. **122**, 49 (2002).

[5] T. Kimura, S. Kawamoto, I. Yamada, M. Azuma, M. Takano, and Y. Tokura, Phys. Rev. B **67**, 180401(R) (2003).

[6] A. Moreira dos Santos, A. K. Cheetham, T. Atou, Y. Syono, Y. Yamaguchi, K. Ohoyama, H. Chiba, and C. N. R. Rao, Phys. Rev. B **66**, 064425 (2002).

[7] D. H. Templeton and L. K. Templeton, Acta Crystallogr., Sect. A: Cryst. Phys., Diffr., Theor. Gen. Crystallogr. **38**, 62 (1982).

[8] V. E. Dmitrienko, Acta Crystallogr., Sect. A: Found. Crystallogr. **39**, 29 (1983).

[9] M. Blume, J. Appl. Phys. **57**, 3615 (1985).

[10] D. Gibbs, D. R. Harshman, E. D. Isaacs, D. B. McWhan, D. Mills, and C. Vettier, Phys. Rev. Lett. **61**, 1241 (1988).

[11] K. D. Finkelstein, Q. Shen, and S. Shastri, Phys. Rev. Lett. **69**, 1612 (1988).

[12] Y. Murakami, H. Kawada, H. Kawata, M. Tanaka, T. Arima, Y. Moritomo, and Y. Tokura, Phys. Rev. Lett. **80**, 1932 (1998).

[13] Y. Murakami, J. P. Hill, D. Gibbs, M. Blume, I. Koyama, M. Tanaka, H. Kawata, T. Arima, Y. Tokura, K. Hirota, and Y. Endoh, Phys. Rev. Lett. **81**, 582 (1998).

[14] C.-H. Yang, T. Y. Koo, S.-H. Lee, C. Song, K.-B. Lee, and Y. H. Jeong, Europhys. Lett. **74**, 348 (2006).